Journal of Applied Polymer Science

Viscoelastic Properties and Filler Dispersion in Carbon Black-Filled and Silica-Filled Cross-Linked Natural Rubbers

Atsushi Kato,[1] Yuko Ikeda,[2] Ryota Tsushi,[2] Youta Kokubo[2]

[1]Strategic Service Promotion Department, NISSAN ARC, LTD., 1 Natsushima-cho, Yokosuka 237-0061, Japan

[2]Graduate School of Science and Technology, Kyoto Institute of Technology, Hashigami-cho, Matsugasaki, Sakyo-ku, Kyoto 606-8585, Japan

Correspondence to: A. Kato (E-mail: kato@nissan-arc.co.jp)

ABSTRACT: The activation energies ($\Delta E_{J'}$ and $\Delta E_{J''}$) calculated from the temperature dependence of the storage compliance (J') and the loss compliance (J'') of carbon black (CB)-filled, hydrophobic silica- and hydrophilic silica-filled cross-linked natural rubbers (NRs) were found to be less than 15 kJ mol^{-1}, which corresponds to the physical range of van der Waals interaction. The results of three-dimensional-transmission electron microscopy measurements indicate that the closest distance (d_p) between the two neighboring nanofiller aggregates centers decreased sharply with increasing nanofiller loading and tended to become constant at a nanofiller loading of around 30 phr or higher. For all samples examined, there were two regions related to the elastic deformation energy, and the critical d_p value between the two regions was in the order of CB > hydrophobic silica = hydrophilic silica. Additionally, $\Delta E_{J'}$ developed in the region of longer d_p than that of $\Delta E_{J''}$. On the other hand, $\Delta E_{J''}$ occurred after the formation of the filler network and was larger than $\Delta E_{J'}$. $\Delta E_{J''}$ is assumed to be related to slippage of the junction and the rearrangement of the nanofiller network. Therefore, the dependence of $\Delta E_{J'}$ and $\Delta E_{J''}$ on d_p suggests that the interaction layer between the nanofiller and NR has at least two energy levels. © 2013 Wiley Periodicals, Inc. J. Appl. Polym. Sci. 130: 2594–2602, 2013

KEYWORDS: composites; cross-linking; elastomers; morphology; viscosity and viscoelasticity

Received 12 March 2013; accepted 26 April 2013; Published online 29 May 2013

DOI: 10.1002/app.39487

INTRODUCTION

Various research results have so far been reported regarding the thickness of bound rubber. For example, Nishi[1] used pulsed nuclear magnetic resonance (NMR) to investigate the relaxation time constant T_2 caused by multiple interactions between different spins of rubber molecules in carbon black (CB)-filled rubber. He measured T_2 of CB gels formed by kneading different types of CB (SAF, HAF, and SRF) and natural rubber (NR) and estimated the thickness of the glassy layer, that is, short T_2 component, in bound rubber to be 0.6–4.3 nm. Recently, Litinov et al.[3] studied CB-filled ethylene propylene diene terpolymer (EPDM) vulcanizates using solid-state NMR and mechanical testing. Their results revealed that a very thin layer (thickness $\leq$ 0.6 nm) consisting of strong immobilized EPDM chain fragments on the CB surface formed a quasi-permanent CB network in the rubber matrix. Based on the measured viscoelasticity of CB-filled rubber, Smitt[2] estimated the thickness of the glassy layer around CB to be 2 nm. Nakajima and Nishi[4] used an atomic force microscope (AFM) to measure the force-volume of CB-filled NR vulcanizates. They reported that bound rubber had a two-layer structure consisting of a glassy layer of about a few (2–3) nm in thickness and an uncured rubber layer of about several (6–7) nm in thickness. They also showed that both layers exhibited an elastic modulus higher than that of the matrix rubber. We have found that the critical value of d_p is approximately 3 nm. Based on our investigations, the tendency for d_p to become constant at a CB loading of 30 phr or higher corresponds well with the tendency for volume resistivity to become nearly constant in the same CB loading range.[5–10] This correspondence is further evidence of the formation of a CB network. In this regard, based on the results of AFM observations of CB-filled elastomers, Yurekli et al.[11] reported that a CB network formed once the filler loading exceeded a level of 9 volume % (20 phr). That result is entirely consistent with our findings.

Considering the aforementioned results, we hypothesized a model[12] of the CB/NR interaction layer as shown in Figure 1. The upper right figure shows the relation between the potential energy at the CB/NR interface and the distance from CB. For example, d_p, d_α, and d_β indicate points of change in potential energy closer to CB. Among them, d_p is presumably the most stable energy position equivalent to d_p obtained by three-

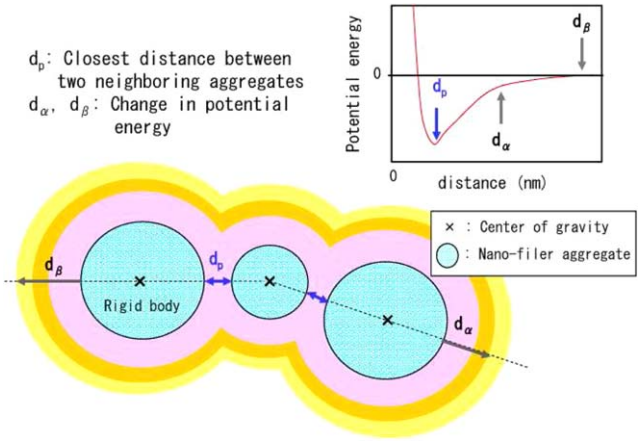

Figure 1. Nanofiller/rubber interface layer. [Color figure can be viewed in the online issue, which is available at wileyonlinelibrary.com.]

dimensional-transmission electron microscopy (3D-TEM). It is reasonable to assume that a layer ranging in depth from a minimum of 1.5 nm to a maximum of approximately 3 nm from the CB particle surface corresponds to the thickness of the CB/NR interaction layer immobilized by the CB filler. In this regard, a d_p value of a few nm corresponds to the thickness of the NR glassy layer around CB as found by Nakajima and Nishi[4] based on pulsed NMR and AFM measurements.

In silica-filled rubber compounds, the hydrophilic siloxane and silanol groups on the silica surface result in strong filler–filler interactions due to strong hydrogen bonds and weak van der Waals bonds.[13–15] As a result, it is much more difficult to disperse silica in rubber compounds than CB. Silane coupling agents are used to improve silica filler dispersion and to prevent adsorption of curatives on the silica surface, which is believed to increase the reinforcing effect of particulate silica on rubber compounds.[13,16] The increased filler concentration induces filler–filler interactions, which promote the formation of filler agglomerates. Accordingly, high filler–filler interactions result in an inhomogeneous filler distribution, problems of poor processing and poor appearance, and inferior properties, for example, an increasing amount of aggregates causes the tensile properties of rubber composites to decline.[16–19] Interaction between the polymer matrix and the filler reduces opportunities for agglomeration.

It is well known that bound rubber is produced in the process of mixing reinforcing fillers such as CB and silica into rubber. The filler is surrounded by bound rubber consisting mainly of polymer phases of different molecular mobility.[20–22] CB in particular disperses in the rubber matrix not as separate primary particles but as aggregates consisting of 5–10 primary particles together. It is believed that a secondary network of polymer chains forms that connects filler particles.[23–27] This transient network is probably the reason for the marked enhancement observed in viscoelastic properties. The transient network also produces rubber-like behavior in a certain range of frequences.[24] Filler networking in elastomer composites can be analyzed by TEM, flocculation, and dielectric investigations. TEM observation provides a limited microscopic view of the filler network morphology. This is mainly due to the spatial interpenetration of neighboring flocculated filler clusters.[27] Flocculation studies focusing on the small strain mechanical response of uncrosslinked composites during heat treatment (annealing) have shown that a relative movement of particles takes place, depending on the particle size, molecular mass of the polymer, and polymer-filler and filler–filler interactions. This provides strong experimental evidence for a kinetic cluster–cluster aggregation mechanism of filler particles in the rubbery matrix that results in the formation of a filler network.[28] Dielectric investigations have revealed that charge transport above the percolation threshold is limited by a hopping or tunneling mechanism of charge carriers across a small gap on the order of 1 nm between CB particles.[29]

In this study, dynamic mechanical properties were measured to investigate the interactions between CB/NR, hydrophobic silica/NR and hydrophilic silica/NR. The dispersions of CB, hydrophobic silica and hydrophilic silica aggregates in the NR matrix were evaluated by using 3D-TEM. The CB/NR, hydrophobic silica/NR and hydrophilic silica/NR interactions were investigated in terms of the relationship between the activation energy of the viscoelastic properties and the closest distance between the centers of gravity of CB, hydrophobic silica and hydrophilic silica aggregates.

EXPERIMENTAL

Sample Preparation Method

The compounding recipes of the CB-filled sulfur NR vulcanizates investigated in this work are given in Table I. The only

Table I. Recipes of CB-Filled NR Compounds[a]

Sample	CB0	CB5	CB10	CB20	CB30	CB40	CB50	CB60	CB80
Ingredients/phr[b]: NR (RSS#1)	100	100	100	100	100	100	100	100	100
Stearic acid (ST)	2	2	2	2	2	2	2	2	2
Active ZnO	1	1	1	1	1	1	1	1	1
CBS[c]	1	1	1	1	1	1	1	1	1
Sulfur	1.5	1.5	1.5	1.5	1.5	1.5	1.5	1.5	1.5
Carbon black (CB)[d]	0	5	10	20	30	40	50	60	80

[a] Curing conditions: 140°C, 15 min under 9.8–14.7 MPa.
[b] Parts by weight per 100 parts by weight of rubber.
[c] N-cyclohexyl-2-benzothiazole sulfenamide
[d] HAF (N330) from Tokai Carbon, grade, dried at 120°C for 2 h.

Applied Polymer SCIENCE

Table II. Recipes for Preparation of Hydrophobic and Hydrophilic Silica-Filled Peroxide Cross-Linked NR[a]

Sample	RX0	RX10	RX20	RX30	RX40	RX60	RX80
NR	100	100	100	100	100	100	100
DCP[b] (phr[c])	1	1	1	1	1	1	1
Silica RX[d] (phr)	0	10	20	30	40	60	80
Sample	VN0	VN 10	VN 20	VN 30	VN 40	VN 60	VN 80
NR	100	100	100	100	100	100	100
DCP[b] (phr[c])	1	1	1	1	1	1	1
Silica RX[e] (phr)	0	10	20	30	40	60	80

[a] Cross-linking conditions: 30 min at 155°C under 9.8–14.7 MPa.
[b] Dicumyl peroxide.
[c] Parts by weight per 100 parts by weight of rubber.
[d] AEROSIL® RX200 (trimethyl silyl group treated silica, average radius = ca. 12 nm) from Evonik Degussa Japan.
[e] Nipsil VN-3 (average primary diameter = ca. 16 nm) from Tosoh Silica Corporation.

ingredient changed in this series of vulcanizates was the amount of CB loading, which was varied from 0 to 80 phr (grams of additive per 100 g of rubber). The quantities of the other compounding agents were all the same; 2 phr of stearic acid, 1 phr each of active zinc oxide (ZnO) and *N*-cyclohexyl-2-benzothiazole sulfenamide, and 1.5 phr of sulfur. The ZnO particles were submicron in size (ca. 0.1 μm).[30] A hot vulcanizing press provided by Gonno Hydraulic Press Manufacturing was used in the vulcanization process. Vulcanization was performed under pressure of 9.8–14.7 MPa at 413 K for 15 min in a compression mold.

The recipes for the preparation of the hydrophobic and hydrophilic silica-filled cross-linked NR samples examined in this study are shown in Table II. The only ingredient changed in this series of samples was the silica loading, which was varied from 0 to 80 phr. The quantity of the dicumyl peroxide cross-linking agent was identical in all samples at 1 phr. Raw rubber and the compounding agents were first kneaded in a two-roller mixer and then subjected to pressure of 9.8–14.7 MPa at 155°C for 30 min, resulting in cross-linked NR samples of approximately 1 mm in thickness. In the following discussion, hydrophobic and hydrophilic silica-filled cross-linked NR samples will be referred to as RX# and VN#, respectively, where # indicates the silica filler loading (phr).

Measurement of Dynamic Viscoelasticity

Storage compliance (J') and loss compliance (J'') were measured under the tensile mode at 20 Hz using a Rheometric Scientific RSA II dynamic mechanical analyzer with a temperature rise rate of 2 K/min from 143 K (−130°C) to 393 K (120°C) in a N_2 gas atmosphere. The size of the original specimens was 3 mm wide, 15 mm long, and 1 mm thick.

3D-TEM Observation

Ultrathin samples for 3D-TEM observation were cut with an ultra-microtome from the cross-linked NR films frozen at the temperature of liquid nitrogen (−198°C). The ultrathin samples were then subjected to a pretreatment process using the NISSAN ACR-SG method[8] to make their thickness uniform and simultaneously smooth the surface. The samples obtained in this way measured approximately 500 nm in length, 500 nm in width, and 200 nm in thickness.

The TEM used was a Tecnai G2 F20 (FEI Company) at an electron beam accelerating voltage of 200 kV. Samples were tilted over a range of angles from −70° to +70°, and image data (tilted images) were continuously obtained in 2° increments. This meant that 71 consecutive tilted images in total were automatically fed into the computer.[6] Using the IMOD software (a program created at Colorado University[31]) installed on the TEM, the consecutive tilted images were then converted to image slices showing the mass-density distribution at each angle. Then, 3D images were reconstructed from the image slices using the Amira software developed by TGS.[32]

RESULTS AND DISCUSSION

Dynamic Mechanical Properties

It is known that a structural change in CB-filled sulfur-cured NR is reflected in its dynamic viscoelastic behavior.[33–35] For example, physical interaction between rubber molecular chains and CB is assumed to be the origin of the Payne effect,[33] which is related to the dependence of the dynamic modulus (E') of filled rubbers on the frequency amplitude. According to McDonald and Hess,[34] E' tends to increase with increasing loading, specific surface area, surface activity, and unit size distribution of CB in the rubbery matrix. They reported that this tendency was closely related to the change in the CB-gel dispersion structure. For resilience, the most important CB variables appear to be CB loading, unit size, unit size distribution, surface activity, and structure. Kraus[35] reported that the loss tangent (tan δ) of CB-filled sulfur-cured butyl rubber increased as a result of increasing the CB loading before the formation of the CB network structure and remained almost constant after the network formed. The aforementioned increase of E' might possibly be attributable to the CB network structure rather than the CB primary particle structure.

Rivin et al.[36] reported that based on their model experimental results for adsorption of 2-methyl-2-octene to CB, 95% of the CB surface area exhibited adhesion by Van der Waals force and the remaining 5% showed a chemical combination. Ban et al.[37] reported that most of the bound rubber of CB- and silica-filled SBR/BR compounds dissolved in chloroform after supersonic wave irradiation. This raises the question of whether any or a small number of cross-linking points are actually present in bound rubber. These findings imply that most of the bound rubber is formed by a physical interaction between the matrix rubber and inorganic filler such as CB. On the other hand, according to Printer et al.,[38] the quantity of bound rubber in CB-filled SBR begins to decrease at temperatures over 373 K (60°C) and most of it disappears by about 423 K (150°C). According to Pérez et al.,[39] the results of modulated

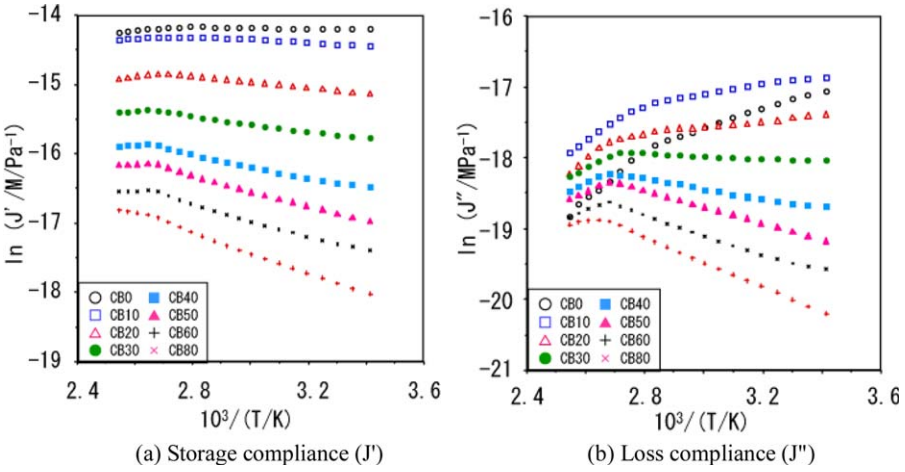

Figure 2. Temperature dependence of storage compliance (J') and loss compliance (J'') of CB-filled NR vulcanizates in the temperature region from 293 to 423 K. (a) Storage compliance (J') and (b) Loss compliance (J''). [Color figure can be viewed in the online issue, which is available at wileyonlinelibrary.com.]

temperature differential scanning calorimetry measurements revealed that the thermal behavior of bound rubber in CB-filled and silica-filled SBR/NBR was reversible in the temperature region from room temperature to 423 K (150°C). Considering these results, bound rubber containing CB aggregates and the CB network probably disappears partially or almost entirely at higher temperatures. It is believed that CB aggregates and the CB network are destroyed and their fragments are rearranged after the reduction and disappearance of bound rubber. During cooling, bound rubber is reproduced reversibly inside and outside the CB aggregates and CB network.

Activation Energy of Viscoelastic Properties

Figures 2, 3, and 4 present Arrhenius plots showing the relationship between the logarithms of the storage compliance (J') and loss compliance (J'') and the reciprocal of temperature ($1/T$) in the temperature range from 293 to 343 K, respectively. All of the tested samples showed a curved relationship for the $1/T$ dependence of J'. Additionally, the samples with filler loadings of 20 phr or higher displayed a negative linear relationship for the $1/T$ dependence of J'' in the lower temperature region.

The activation energies ($\Delta E_{J'}$ and $\Delta E_{J''}$) calculated from these two negative linear relationships are plotted in Figure 5 as a function of the CB or silica loading. The $\Delta E_{J'}$ and $\Delta E_{J''}$ values of nearly all the samples are less than 15 kJ mol^{-1}, corresponding to the physical range of van der Waals interaction.[40,41] The relationship between $\Delta E_{J'}$ and the CB or hydrophobic silica loading is nearly linear. This linearity is assumed to be attributable to the interaction between the filler and rubber matrix. In contrast, the $\Delta E_{J'}$ of hydrophilic silica-filled cross-linked NR increases with an increase in hydrophilic silica loading up to 20 phr and becomes almost constant at 30 phr or higher. Considering that a hydrophilic silica network forms at 30 phr or higher,[15] this constant $\Delta E_{J'}$ is probably related to slippage between the NR molecular chains near the filler network junction, which leads to rearrangement of the network.

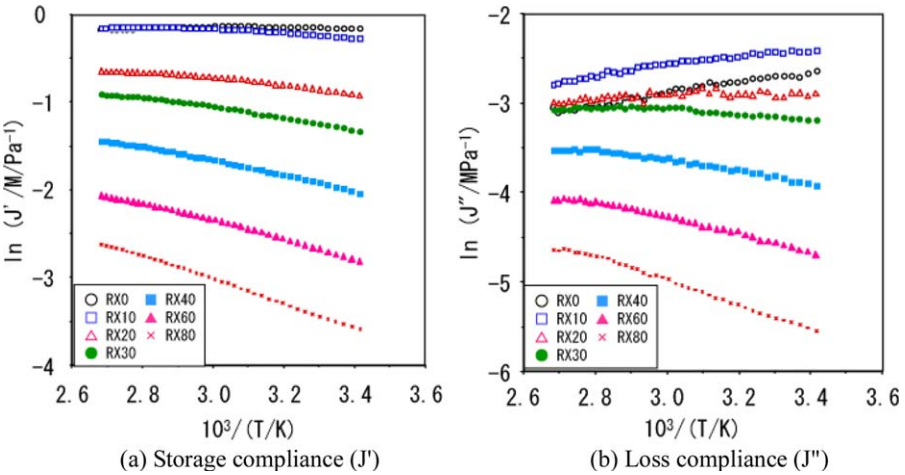

Figure 3. Temperature dependence of storage compliance (J') and loss compliance (J'') of hydrophobic silica-filled NR vulcanizates in the temperature region from 293 to 423 K. (a) Storage compliance (J') and (b) Loss compliance (J''). [Color figure can be viewed in the online issue, which is available at wileyonlinelibrary.com.]

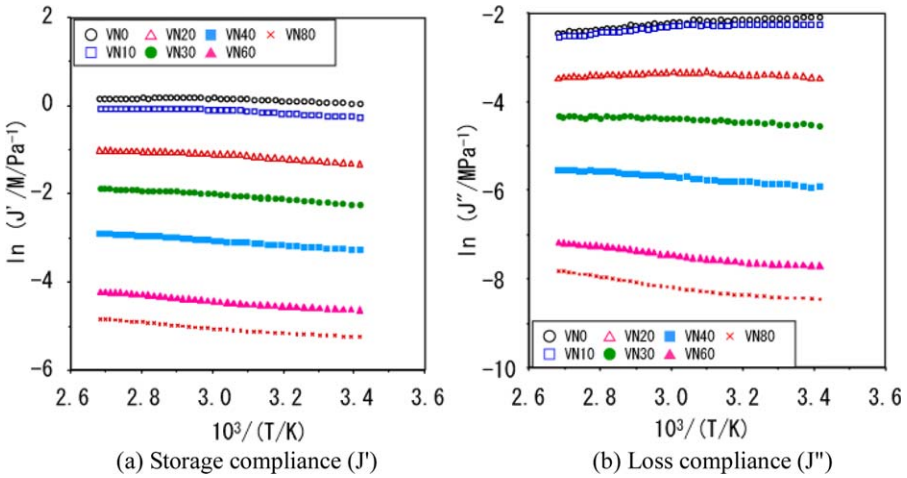

Figure 4. Temperature dependence of storage compliance (J') and loss compliance (J'') of hydrophilic silica-filled NR vulcanizates in the temperature region from 293 to 423 K. (a) Storage compliance (J') and (b) Loss compliance (J''). [Color figure can be viewed in the online issue, which is available at wileyonlinelibrary.com.]

The other activation energy $\Delta E_{J''}$ occurred at CB or hydrophobic silica loadings of 20 phr or higher and tended to increase almost linearly with a higher filler loading. It is inferred from these results that this tendency is ascribable to the structure of the aggregates/agglomerates. In this connection, Caoa et al.[42] have pointed out that the activation energy of thermally induced percolation in CB-filled high-density polyethylene (HDPE) is markedly higher than the viscous flow or molecular relaxation in the polymer matrix. On the other hand, in this study, $\Delta E_{J''}$ of hydrophilic silica-filled cross-linked NR increased with an increase in filler loading up to 40 phr and became almost constant at higher loadings. This result also suggests the occurrence of slippage between the NR molecular chains near the network junction at loadings of 40 phr or higher. The relationship between $\Delta E_{J'}$ and $\Delta E_{J''}$ of the samples is shown in Figure 6. In CB-filled NR vulcanizates and hydrophobic silica-filled cross-linked NR, $\Delta E_{J''}$ increased linearly with an increase in $\Delta E_{J'}$, whereas in hydrophilic silica-filled cross-linked NR, $\Delta E_{J''}$ was not affected by $\Delta E_{J'}$. As aforementioned, it is assumed that the former and the latter tendencies are closely related to the interaction between the filler and NR matrix and slippage between the NR molecular chains near the network junction.

Filler Dispersion

To make the dispersion state of CB and silica easier to understand, an image processing technique[5–10,12,15,43–45] was applied to 3D-TEM images of CB30, RX30, and VN30 from which the Zn compounds had been removed, and the results obtained are shown in Figure 7. An aggregate, in which a few or several CB and silica particles are in contact, is painted by a color, and the adjacent CB and silica aggregates are shown in different colors to make them easier to recognize. Because 3D-TEM provides information along the depth direction of the samples, the different in the dispersion state of the CB and silica aggregates is obvious at a glance. Primary filler particles of 10–30 nm in size and larger aggregates packed closely together are clearly

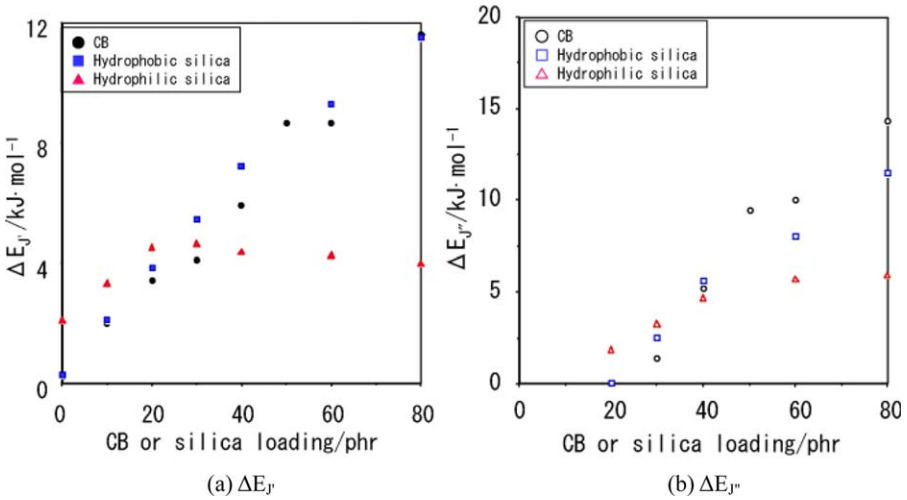

Figure 5. Dependence of activation energies ($\Delta E_{J'}$ and $\Delta E_{J''}$) on CB or silica loading. (a) $\Delta E_{J'}$ and (b) $\Delta E_{J''}$. [Color figure can be viewed in the online issue, which is available at wileyonlinelibrary.com.]

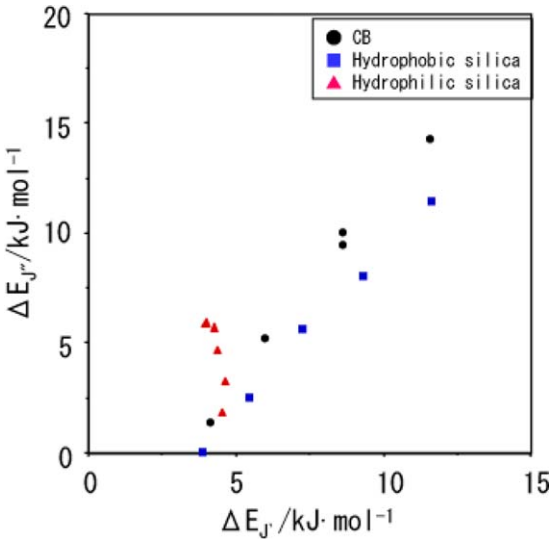

Figure 6. Relationship between $\Delta E_{J'}$ and $\Delta E_{J''}$. [Color figure can be viewed in the online issue, which is available at wileyonlinelibrary.com.]

observable. The closest distance (d_p) between the centers of gravity of the nanofiller aggregates can be found as a 3D parameter from the image processing results in the figure. We provisionally define a nanofiller aggregate as a collection of adjacent primary nanofiller particles within a distance of approximately 1 nm, which is the resolution of the 3D-TEM apparatus used.[5–10,12,15,43–45] The definition of d_p is shown schematically in Figure 8. The nanofiller aggregates are represented as circles (spheres) for convenience. The distance between the two aggregates along a line connecting their centers of gravity is defined as d_p. Figure 9 shows the average values of d_p as a function of the CB or silica loading. The results indicate that d_p decreased sharply with increasing nanofiller loading and tended to become constant at a nanofiller loading of around 30 phr or higher. This tendency suggests that the nanofiller aggregates were nonuniformly dispersed in the rubber matrix in the low nanofiller loading range below 30 phr and that they became closely and uniformly distributed as the nanofiller loading was increased.[5,6,8,10,15] It also implies that the nanofiller aggregates became linked and formed a nanofiller network at certain critical values of d_p in a nanofiller loading range of about 30 phr or higher. The d_p values of CB and silica were approximately 3 nm and 1.3 nm, respectively.

The dependence of the activation energies ($\Delta E_{J'}$ and $\Delta E_{J''}$) on d_p is shown in Figure 10. The $\Delta E_{J'}$ vs. d_p lines of CB and hydrophobic silica show a knick at d_p = ca. 3 nm and ca. 2 nm, respectively. While the relationship between d_p and $\Delta E_{J'}$ of hydrophilic silica is not sufficiently clear, it appears that $\Delta E_{J'}$ of

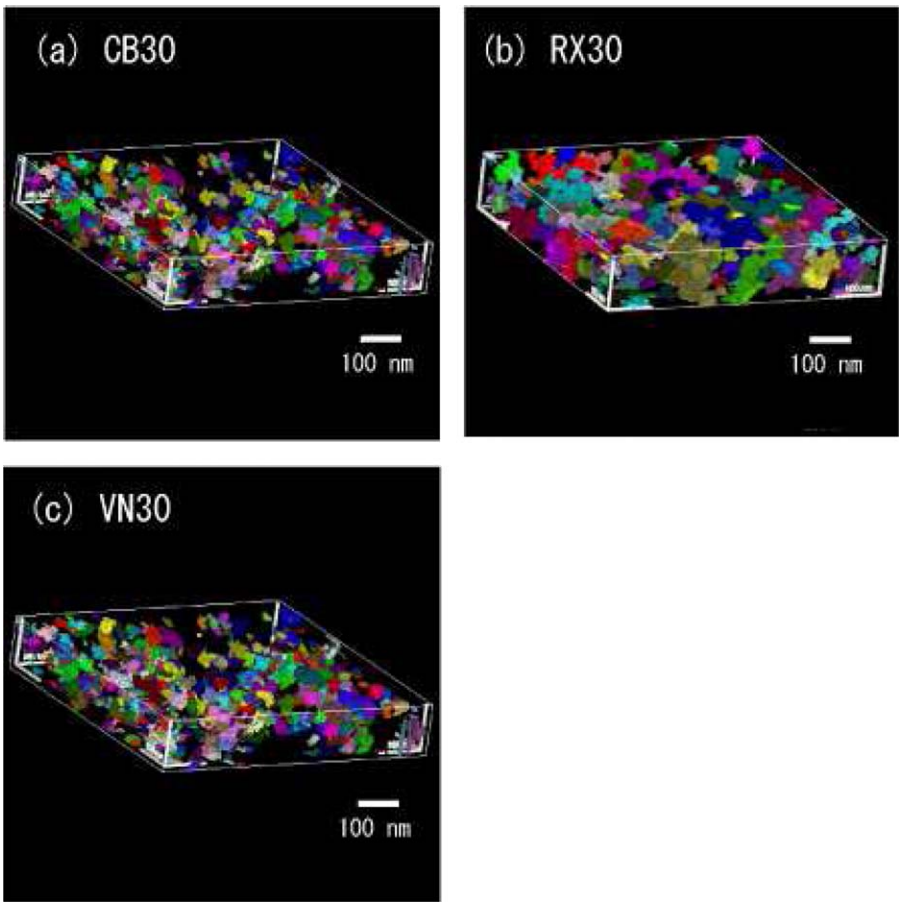

Figure 7. 3D-image analysis results for CB30, RX30, and VN30. (a) CB30, b) RX30, and (c) VN30. [Color figure can be viewed in the online issue, which is available at wileyonlinelibrary.com.]

Applied Polymer SCIENCE

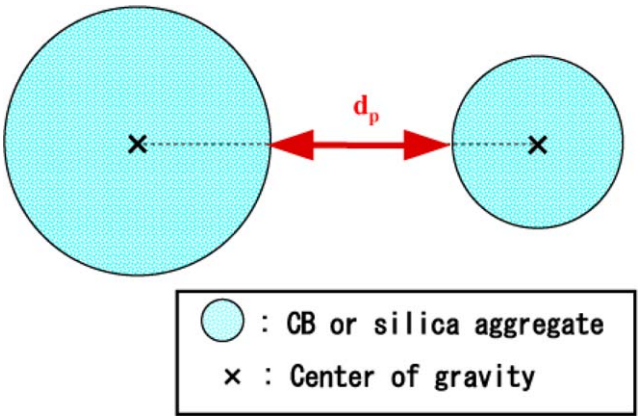

Figure 8. Definition of closest distance (d_p) between two neighboring CB or silica aggregates as a 3D parameter. [Color figure can be viewed in the online issue, which is available at wileyonlinelibrary.com.]

hydrophilic silica became constant below d_p = ca. 2 nm and decreased with an increase in d_p over d_p = ca. 2 nm. These results reveal that for the three samples there are two regions which are related to the elastic deformation energy and that the critical d_p value of the two regions is in the order of CB > hydrophobic silica = hydrophilic silica. Additionally, $\Delta E_{J'}$ occurred from the region of a longer d_p than that of $\Delta E_{J''}$. Presumably, $\Delta E_{J'}$ reflects the ability of the nanofiller reinforcement and is closely related to the interaction between the nanofiller and NR. This interaction might be with an immobilized NR layer such as bound rubber, which enhances elasticity.

On the other hand, $\Delta E_{J''}$ occurred after the formation of the filler network and was larger than $\Delta E_{J'}$. Specifically, the decreases of $\Delta E_{J''}$ for hydrophobic silica and hydrophilic silica are curved at d_p = ca. 3.2 nm, ca. 2.5 nm, and ca. 2.7 nm, respectively. These results suggest that $\Delta E_{J''}$ is related to slippage of the junction and the rearrangement of the nanofiller network. Therefore, the dependence of $\Delta E_{J'}$ and $\Delta E_{J''}$ on d_p suggests that the interaction layer between the nanofiller and NR has at least two energy levels.

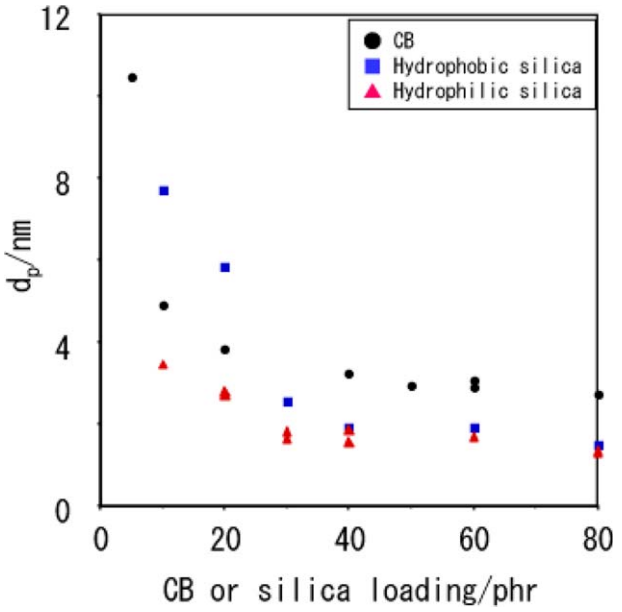

Figure 9. Dependence of d_p on CB or silica loading. [Color figure can be viewed in the online issue, which is available at wileyonlinelibrary.com.]

CONCLUSIONS

Regarding the relationship between the logarithms of the storage compliance (J') and loss compliance (J'') and the reciprocal of temperature ($1/T$) in the temperature range from 293 to 343 K, the activation energies ($\Delta E_{J'}$ and $\Delta E_{J''}$) were calculated from these negative linear relationships. The $\Delta E_{J'}$ and $\Delta E_{J''}$ values of nearly all the samples were found to be less than 15 kJ mol^{-1}, corresponding to the physical range of van der Waals interaction. The linear relationship between $\Delta E_{J'}$ and the CB or hydrophobic silica loading is, therefore, assumed to be attributable to the interaction between the filler and rubber matrix. The $\Delta E_{J'}$ of hydrophilic silica-filled cross-linked NR increased with an increase in filler loading at 20 phr or less and became almost constant at loadings of 30 phr or higher. Considering that a

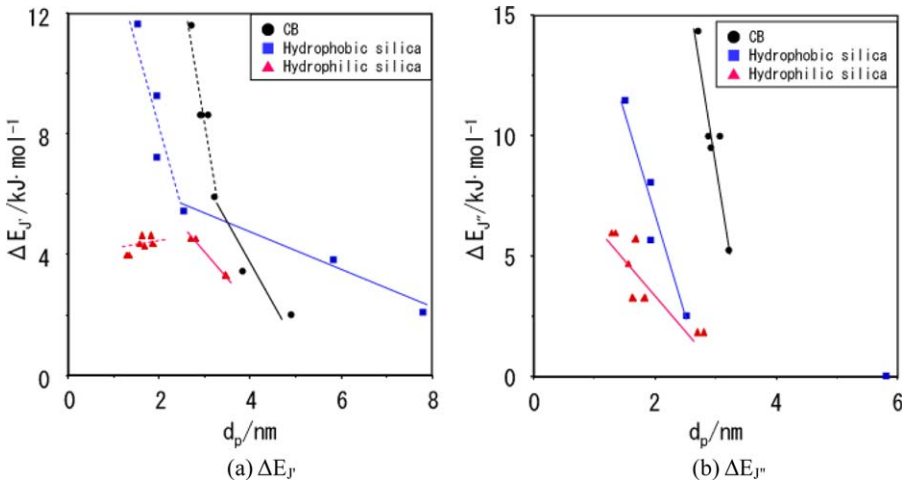

Figure 10. Dependence of activation energies ($\Delta E_{J'}$ and $\Delta E_{J''}$) on d_p. The dotted and solid lines are for the eyes' guides. (a) $\Delta E_{J'}$ and (b) $\Delta E_{J''}$. [Color figure can be viewed in the online issue, which is available at wileyonlinelibrary.com.]

hydrophilic silica network forms at loadings of 30 phr or higher, this constant ΔE_f behavior is probably related to slippage between the NR molecular chains near the filler network junction, which leads to rearrangement of the network. In contrast, $\Delta E_{f''}$ occurred at CB or hydrophobic silica loadings of 20 phr or higher and tended to increase almost linearly with a higher filler loading. It is inferred from these results that this tendency is ascribable to the structure of their aggregates/agglomerates. In CB-filled NR vulcanizates and hydrophobic silica-filled cross-linked NR, $\Delta E_{f''}$ increased linearly with an increase in ΔE_f, whereas in hydrophilic silica-filled cross-linked NR, $\Delta E_{f''}$ was not affected by ΔE_f. It is assumed that the former and the latter results are closely related to the interaction between the filler and NR matrix and slippage between the NR molecular chains near the network junction.

The results of 3D-TEM measurements indicated that the closest distance (d_p) between the centers of gravity of nanofiller aggregates decreased sharply with increasing nanofiller loading and tended to become constant at a nanofiller loading of around 30 phr or higher. It implies that the nanofiller aggregates became linked and formed a nanofiller network at certain critical values of d_p in a nanofiller loading range of about 30 phr or higher. ΔE_f of CB decreased linearly with an increase in d_p below and over d_p = ca. 3 nm. ΔE_f of hydrophobic silica decreased linearly with an increase in d_p below and over d_p = ca. 2 nm. While the relationship between d_p and ΔE_f of hydrophilic silica is not sufficiently clear, it appears that ΔE_f of hydrophilic silica becomes constant below d_p = ca. 2 nm and decreases with an increase in d_p over d_p = ca. 2 nm. These results reveal that for all the samples examined there were the two regions which were related to the elastic deformation energy and that the critical d_p value of the two region was in the order of CB > hydrophobic silica = hydrophilic silica. On the other hand, $\Delta E_{f''}$ occurred after the formation of the filler network and was larger than ΔE_f. Specifically, the $\Delta E_{f''}$ values of CB, hydrophobic silica and hydrophilic silica decreased linearly with increasing d_p in the d_p regions from 2.7 to 3.2 nm, from 1.5 to 2.5 nm, and from 1.3 to 2.7 nm, respectively. These results suggest that $\Delta E_{f''}$ is related to slippage of the junction and the rearrangement of the nanofiller network. Therefore, the dependence of ΔE_f and $\Delta E_{f''}$ on d_p suggests that the interaction layer between the nanofiller and NR has at least two energy levels.

ACKNOWLEDGMENTS

The authors would like to thank Emeritus Professor S. Kohjiya of Kyoto University, and T. Suda, H. Sawabe, J. Shimanuki, M. Hashimoto, M. Gonda, and A. Isoda of NISSAN ARC, LTD., and Y. Kasahara of the Kyoto Institute of Technology for their valuable cooperation and advice.

REFERENCES

1. Nishi, T. J. *Polym. Sci. Polym. Phys. Ed.* **1974**, *12*, 685.
2. Smit, P. P. A. *Rubber Chem. Technol.* **1968**, *41*, 1194.
3. Litvinov, V. M.; Orza, R. A.; Klüppel, M.; van Duin, M.; Magusin, P. C. M. *M. Macromolecules* **2011**, *44*, 4887.
4. Nakajima, K.; Nishi, T. In Current Topics in Elastomers Research. Recent Developments in Rubber Research using Atomic Force Microscopy; Bhomik, A. K., Ed.; CRC Press: Boca Raton, **2008**; Chapter 21, p 579.
5. Kohjiya, S.; Ikeda, Y.; Kato, A. In Current Topics in Elastomers Research. Visualization of Nano-Filler Dispersion and Morphology in Rubbery Matrix by 3D-TEM; Bhowmick, A. K., Ed.; CRC Press: Boca Raton, **2008**; Chapter 19, p 543.
6. Kohjiya S.; Kato A.; Ikeda Y. *Prog. Polym. Sci.* **2008**, *33*, 979.
7. Kohjiya, S.; Kato, A.; Suda, T.; Shimanuki, J.; Ikeda, Y. *Polymer* **2006**, *47*, 3298.
8. Kato, A.; Shimanuki, J.; Kohjiya, S.; Ikeda, Y. *Rubber Chem. Technol.* **2006**, *79*, 653.
9. Ikeda, Y.; Kato, A.; Shimanuki, J.; Kohjiya, S.; Tosaka, M.; Poompradub, S.; Toki, S.; Hsiao, B. S. *Rubber Chem. Technol.* **2007**, *80*, 251.
10. Kato, A.; Ikeda, Y.; Kohjiya, S. In Polymer Composites: Macro- and Microcomposites. Carbon Black-Filled Natural Rubber Composites: Physical Chemistry and Reinforcing Mechanism; Thomas, S.; Joseph, K.; Malhotra, S. K.; Goda, K.; Streekala, M. S., Eds.; WILEY-VCH Verlag GmbH & Co. KGaA: Boscher, **2012**; Vol. *1*, Chapter 17, p 515.
11. Yurekli, K.; Krishnamooti, R.; Tse, M. F.; McElrath, K. O.; Tsou, A. H.; Wang, H. C. J. *Polym. Sci. Part B: Polym. Phys.* **2001**, *39*, 256.
12. Kato, A.; Ikeda, Y.; Tsushi, R.; Kokubo, Y.; Kojima, N. *Colloid Polym. Sci.*, to appear; DOI 10.1007/s00396-013-2948-3.
13. Plueddemann, E. P., Ed., Silane Coupling Agents; Plenum Press: New York, **1982**.
14. Chabert, E.; Dendievel, R.; Gauthier, C.; J. Cavailė, J. Y. *Compos. Sci. Technol.* **2004**, *64*, 309.
15. Kato, A.; Ikeda, Y.; Kasahara, Y.; Shimanuki, J.; Suda, T.; Hasegawa, T.; Sawabe, H.; Kohjiya, S. *J. Opt. Soc. Am. B 25* **2008**, 1602.
16. Scurati, A.; Manas-Zloczower, I. *Rubber Chem. Technol.* **2001**, *75*, 725.
17. Poh, B. T.; Keok, C. P.; Lim, G. H. *Eur. Polym. J.* **1995**, *31*, 223.
18. Poh, B. T.; Ismail, H.; Tan, K. S. *Polym. Test.* **2002**, *21*, 801.
19. da Silva, A. L. N.; Rocha, M. M. C. G.; Moraes, M. A. R. C.; Valente, C. A. R.; Coutinho, F. M. B. *Polym. Test.* **2002**, *21*, 57.
20. Fujiwara, S.; Fujimoto, K. *Rubber Chem. Technol.* **1971**, *44*, 1273.
21. Kaufman, S.; Slichter, W. P.; Davis, D. D. *J. Polym. Sci. A2* **1971**, *8*, 829.
22. O'Brien, J.; Cassshell, J. E.; Wardell, G. E.; McBriety, V. J. *Macromolecules* **1976**, *9*, 653.
23. Zhang, Q.; Archer, L. *Langmuir* **2002**, *18*, 10435.
24. Zhang, Q.; Archer, L. *Macromolecules* **2004**, *37*, 1928.
25. Steinstein, S. S.; Zhu, A. *Macromolecules* **2002**, *35*, 7262.
26. Zhu, Z.; Thompson, T.; Wang, S. Q.; von Meerwall E. D.; Halasa, A. *Macromolecules* **2005**, *38*, 8816.
27. Fukahori, Y. In Current Topics in Elastomers Research. Mechanism of the Carbon Black Reinforcement of Rubbers;

Bhowmick, A. K., Ed.; CRC Press: Boca Raton, **2008**; Chapter 18, p 517.

28. Klüppel, M. *Adv. Polym. Sci.* **2003**, *164*, 1.
29. Klüppel, M.; Heinrich, G. *Kautsch. Gummi Kunstst.* **2005**, *58*, 217.
30. Japanese Zinc-Demand Society Ed., Zinc Handbook 1977; Nikkan Kogyou Shimbun: Tokyo, **1977**; p 379.
31. Kremer, J. R.; Mastronarde, D. N.; McIntosh, J. R. *J. Struct. Biol.* **1996**, *116*, 71.
32. Detlev S., Malte W., Hans-Christian H. In The Visualization Handbook. A Highly Interactive System for Visual Data Analysis; Hansen, C. D.; Johnson, C. R., Eds.; Elsevier: Amsterdam, **2005**; Chapter 38 Amira, p 749.
33. Payne, A. R.; Whittaker, R. E. *Rubber Chem. Technol.* **1971**, *44*, 440.
34. McDonald, G.; Hess, W. *Rubber Chem. Technol.* **1977**, *50*, 842.
35. Kraus, G. *Rubber Chem. Technol.* **1978**, *51*, 297.
36. Rivin, D.; Aron, J.; Medalia, A. I. *Rubber Chem. Technol* **1968**, *41*, 330.
37. Ban, L. L.; Hess, W. M.; Papazian, L. A. *Rubber Chem. Technol.* **1974**, *47*, 858.
38. Printer, P. E.; McGill, G. R. *Rubber World* **1978**, *30*, 177.
39. Pérez, L. D.; Sierra, L.; Lopez, B. L. *Polym. Eng. Sci* **2008**, *48*, 1986.
40. Heinrich, G.; Klüppel, M., *Kautsch. Gummi Kunstst.* **2004**, *57*, 452.
41. Ladouce-Stelander, L.; Bomal, Y.; Flandin, L.; Labarre, D. *Rubber Chem. Technol.* **2003**, *76*, 145.
42. Caoa, Q.; Songa, Y.; Tana, Y.; Zhenga, Q. *Polymer* **2009**, *50*, 6350.
43. Ikeda, Y.; Kato, A.; Shimanuki, J.; Kohjiya, S. *Macromol. Rapid Commun.* **2004**, *25*, 1186.
44. Ikeda, Y. *Sen'i Gakkaishi* **2005**, *61*, 34.
45. Kohjiya, S.; Kato, A.; Shimanuki, J.; Hasegawa, T.; Ikeda Y. *Polymer* **2005**, *46*, 4440.